Tunneling asymmetries in doped Al-AlO_x-Pb junctions

M. F. Muldoon, R. A. Dragoset, and R. V. Coleman
Department of Physics, University of Virginia, Charlottesville, Virginia 22903
(Received 5 March 1979)

Asymmetries in both the elastic and inelastic electron tunneling components of Al-AlO_x-Pb junctions doped with organic ring compounds have been examined. The barrier shapes and heights and the correlated behavior of the elastic characteristic curves and the inelastic vibrational modes are unusually sensitive to differences in molecular components and the resulting interface structure of the junction. Model barriers fitted with a computer program adequately fit the large variations in $\pm$ bias asymmetry of the elastic tunneling component observed for different molecules. Asymmetries in the inelastic mode intensity generally indicate an agreement with a long-range potential interaction between the molecule and tunneling electron. Enhanced asymmetry in inelastic mode intensity is observed for some cases which also show usually low effective organic barriers and a correlated effect on mode coupling.

I. INTRODUCTION

Tunnel junctions doped with organic impurities have been used for a wide range of studies on the excitation of molecular vibrations via the mechanism of inelastic electron tunneling.[1,2] The inelastic tunneling channel involves the coupling of the tunneling electron to the bonding electrons of the impurity molecule and the excitation of a vibrational mode of the molecule via the electron-phonon coupling in the molecule. A number of theoretical papers[3,4] have developed model calculations for the magnitude and range of this interaction.

Under most doping procedures the molecules are adsorbed on an oxide substrate and both the oxide and molecular layer contribute to the tunneling barrier between the metal electrodes. When dissimilar electrodes are used the difference in work functions results in a charge transfer and the development of an electric field in the barrier which gives rise to a trapezoidal[5] shape for the barrier. The elastic tunneling characteristic will therefore show a natural (±) bias asymmetry reflecting the presence of the trapezoidal barrier. A natural (±) bias asymmetry is also introduced in the inelastic tunneling intensity when the molecules are placed closer to one electrode than to the other. This arises from the spatial location of the interaction potential and the consequent asymmetry in transmission probability for the inelastic tunneling electron when the tunneling direction is reversed. The amount of asymmetry can be related to the range of the interaction potential and has been calculated and compared to experiment by Kirtley *et al.*[4] for benzoic acid doped on AlO_x for a Al-AlO_x-Pb junction.

When a wide range of organic molecules are used to fabricate tunnel junctions a striking variation is observed in the magnitudes and asymmetries of both the elastic and inelastic tunneling components.[6,7] A two-barrier model was previously used by our group in order to compare the elastic behaviors observed for different dopants on both AlO_x and MgO_x tunnel barriers. The resulting variation in effective organic barrier heights was compared for a wide range of compounds and substantial differences were observed for different dopants on both AlO_x and MgO_x. In this paper we have extended this model to a more detailed study of the (±) bias asymmetries and have developed the data and analysis for a complete comparison between both elastic and inelastic junction asymmetries.

II. EXPERIMENTAL TECHNIQUE

The tunneling measurements reported here were taken using aluminum–aluminum-oxide–lead tunnel junctions. The junctions were fabricated in an oil diffusion pumped vacuum system at 10^{-6} Torr using the following sequence of steps. Five thin-film aluminum strips were evaporated from a resistively heated tungsten coil onto a precleaned microscope slide.[8] The slide was transferred from the vacuum to a laminar flow hood where the aluminum strips were oxidized in air for a period of five minutes. Liquid phase doping of the oxidized strips, as initially described by Hansma and Coleman,[9] was accomplished by placing a drop of dopant solution on the strips and immediately spinning off the excess liquid. To complete the junctions, the slide was returned to the vacuum chamber where a strip of lead from a molybdenum boat was evaporated crosswise over the doped aluminum oxide strips.

Dopant solutions were prepared beforehand. The organic solvents used were ethanol, toluene, benzene, and chloroform. Solution concentrations were varied from 0.02 to 1 mg/ml in order to ob-

tain junctions in the resistance range of 200 to 650 Ω. The majority of chemicals and solvents were of spectrograde purity and were obtained from Aldrich and Eastman Chemical companies.

The resistances of the completed junctions were measured at room temperature using a low-voltage ohmmeter. The center junction of each slide was left undoped as a monitor for outside contamination. The resistance is an indication of the amount of material adsorbed onto the oxide surface of the junctions. Clean junctions had a nominal resistance of 15–30 Ω. Junctions were mounted in a sample holder and lowered into a liquid-helium dewar. All measurements were taken at 4.2 K.

The I-V curve is a sum of the elastic and inelastic tunneling contributions to the junction current. Due to the very small relative component of inelastic structure, the measurements of interest include dV/dI vs V and d^2V/dI^2 vs V as well as I vs V.

The inelastic component of the tunneling current appears as a set of peaks in the second derivative, d^2V/dI^2 vs V, curve. Each peak occurs at a voltage V such that $eV=\hbar\omega+\Delta$, where $\hbar\omega$ is the characteristic energy of a vibrational mode in the barrier excited by the tunneling electron and Δ is the superconducting energy gap of the lead electrode. Measurements are obtained by incorporating the junction into a bridge circuit developed after Adler *et al.*[10] A 500-Hz ac modulation voltage with an amplitude of approximately 1 mV is applied to the junction and the first and second derivative curves are then recorded directly using conventional harmonic detection with a lock-in amplifier. Resolution of the second derivative plots, or tunneling spectra, is on the order of 8 cm^{-1}. The I-V curve was recorded by placing a resistor in series with the junction to obtain the current and measuring the junction voltage directly.

When the first and second derivative curves are used to calculate the inelastic asymmetry we use ΔG to represent the increase in conductance that occurs at specific bias voltages $V_i=\hbar\omega_i/e$ due to the onset of the inelastic tunneling channel. In most cases the conductance increase at a given bias voltage is larger when the lead electrode is biased positive than when the lead electrode is biased negative and we use the ratio $\Delta G_-/\Delta G_+$ as a measure of the inelastic asymmetry.

The conductance increases are determined to a good approximation using the peak areas of the d^2V/dI^2 curve in conjunction with the measured junction conductance $G=dI/dV$. The area is related to the conductance and conductance change by

$$A=\int\frac{d^2V}{dI^2}\,dV=\int G^{-3}\frac{d^2I}{dV^2}\,dV\cong G^{-3}\Delta G\,.$$

The conductance G varies by less than 3% over the voltage range of most inelastic peaks so that G^3 may be taken outside the integral with a minimal loss of accuracy. The areas of the peaks are determined graphically using a planimeter. The error involved in this process is the limiting factor in the analysis and is due to the combined effects of planimeter inaccuracy, the presence of noise and difficulty in determining the exact elastic background of the tunneling spectra.

Area asymmetries were measured for selected peaks in the 1–200 mV region and for the C-H stretch peak between 350 and 400 mV. The scatter in the data is large, but is within a range consistent with the error anticipated from the three factors mentioned above. A smooth curve has been drawn to fit these points and points on this curve have then been used in further calculations involving area asymmetry.

III. EXPERIMENTAL RESULTS

A. Elastic tunneling characteristics

The I vs V and dV/dI vs V characteristic curves for Al-AlO$_x$-Pb junctions can be substantially modified by doping with organic molecules. The additional barrier thickness contributed by the layer of molecules increases the zero-bias resistance and modifies the nonlinear characteristic of the junctions at high bias voltages. These modifications are highly variable and depend on the substitutional groups on the organic molecules and the related interaction of the molecule with the aluminum oxide substrate. The doped junctions also show large variations in the (±) bias asymmetry observed in the I vs V and dV/dI vs V curves. These are related to the nonlinear behavior and also reflect the detailed shape of the modified tunnel barrier.

The variety of I vs V and dV/dI vs V behavior observed results from a combination of nonlinearity and (±) bias asymmetry. Representative I vs V curves for Al-AlO$_x$-Pb junctions doped with coronene, 4-cyanobenzoic acid, and perylene-3-COOH are shown in Fig. 1. In all cases the current for Al$^+$ rises more rapidly than for Pb$^+$ but for either bias there are large differences in nonlinearity for the different dopants over a comparable range of bias voltage. The coronene doped junction shows relatively mild nonlinearity with substantial (±) asymmetry developing at voltages above 0.6 V. Junctions doped with 4-cyanobenzoic acid and perylene-3-COOH both develop extreme nonlinearity above 0.3 V and the (±) bias asymmetry is accentuated by asymmetry in the onset of the nonlinear region. In contrast junctions doped with other compounds, for example 3,4-dinitrobenzoic acid, are highly symmetric with substantially less non-

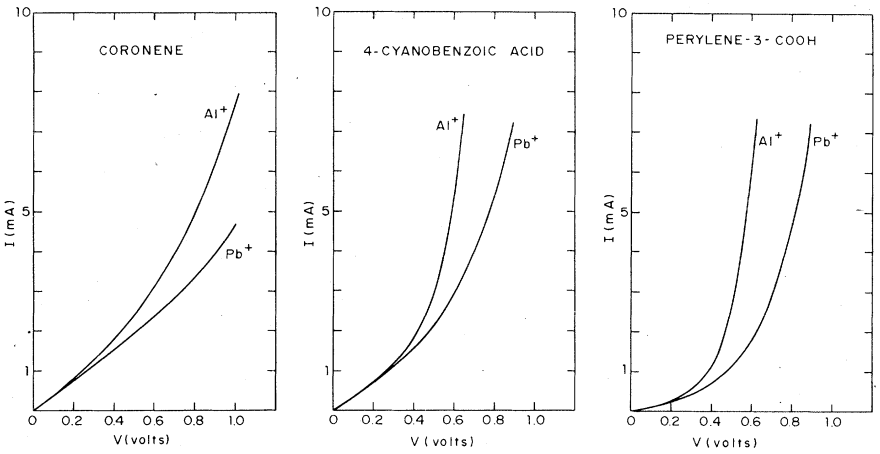

FIG. 1. I vs V curves for Al-AlO_x-Pb junctions doped with coronene, 4-cyanobenzoic acid, and perylene-3-COOH. The curves labeled Pb^+ and Al^+ are taken for opposite bias polarities on the junction and demonstrate the asymmetry in elastic tunneling. The three doping compounds shown represent the range of nonlinear behavior observed for a variety of aromatic ring compounds.

linearity below 1.0 V.

The overall elastic asymmetry of the different doped junctions can also be easily compared using the dynamic resistance dV/dI vs V curves as shown in Fig. 2. The positive and negative bias curves for a given junction are plotted to the same maximum voltage in order to facilitate comparison. Although the data of Fig. 2 have been taken for junctions with different resistances at low bias the dynamic resistance has been calibrated and normalized to the junction resistance at 50 mV. Therefore the relative change in dynamic resistance and the difference in (±) bias asymmetry can be compared for the different compounds. The highly nonlinear junctions with dopants such as perylene-3-COOH and 4-cyanobenzoic acid show a rapid decrease in dynamic resistance with very strong (±) bias asymmetries as shown in Fig. 2(b). Other dopants show a range of behavior with varying degrees of (±) bias asymmetry and examples are shown in Fig. 2(a). The dopants corenene and anthracene-9-carboxylic acid show very similar elastic tunneling characteristics with a pronounced (±) bias asymmetry but a relatively small nonlinear behavior over a 0 to 1-V range as shown for coronene in Fig. 2(a). 3,4-dinitrobenzoic acid shows the least (±) bias asymmetry and also exhibits a weak nonlinear behavior as shown in Fig. 2(a).

The doped junctions with varying degrees of nonlinear behavior can be modeled with a two barrier model to be discussed in Sec. IV A. The bias asymmetries for most junctions can be adequately fitted with a single set of barrier parameters and are represented by effective organic barrier heights in the range 3–9 eV. The dopants which induce extreme nonlinear behavior require very low effective barrier heights and the extreme (±) bias asymmetries are more difficult to fit with a single set of model barrier parameters although fair overall fits can be obtained. Effective organic barrier heights of 1 eV or less are required in these cases.

In addition to the features of the elastic tunnel characteristics summarized above, the inelastic components observed in the d^2V/dI^2 vs V curves have also been studied for both (±) bias asymmetries and for variations in peak intensity and background. The inelastic behavior shows substantial variation for different dopants, but the analysis indicates that these differences are not in general correlated with the variations in elastic characteristics. Representative experimental results will be presented in Sec. III B.

B. Asymmetry in inelastic peak intensities

The inelastic tunneling spectra have been measured for the same organic dopants as used in the studies of elastic tunneling characteristics. The quantity experimentally recorded is d^2V/dI^2 and includes contributions from both the inelastic channel due to phonon excitation and the elastic channel giving rise to the background. The large asymmetries and nonlinear behavior in the elastic tunneling contribute to major changes in the overall background behavior of d^2V/dI^2 for the different dopants as is evident in the spectra shown in Figs. 3–7.

The inelastic spectra have been recorded for both the Pb and the Al at positive voltage and all compounds follow the same general pattern although at high bias voltages the elastic background can show substantial variation. In all cases the inelastic peak intensity due to phonon excitation is smaller for the spectrum recorded with the aluminum electrode positive than for the lead electrode positive. In order to make a quantitative comparison to theory the data must be converted to d^2I/dV^2 and the area under each peak calculated. This

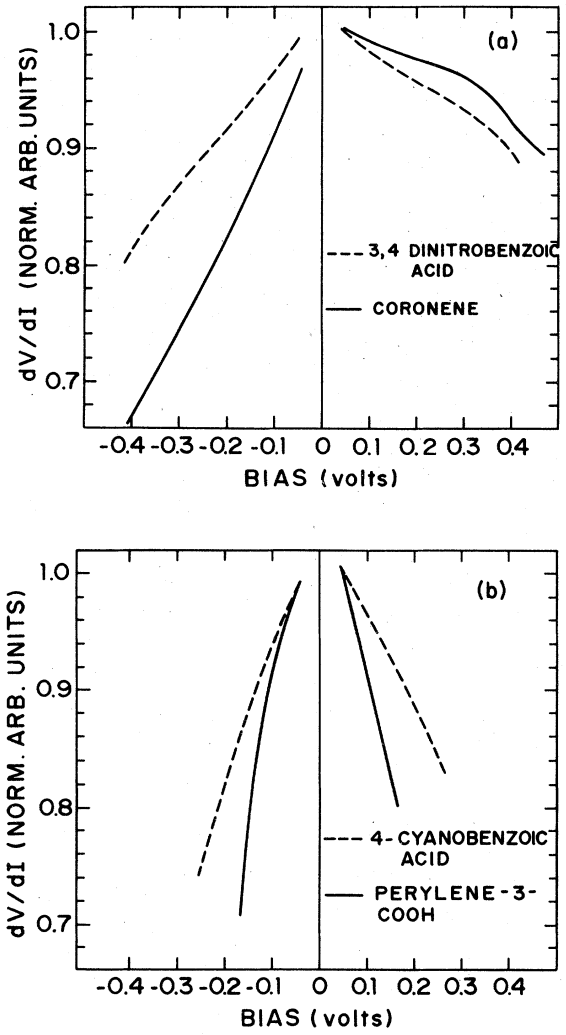

FIG. 2. Normalized dynamic resistance vs voltage plots are shown for representative doping compounds. (a) Coronene and 3,4-dinitrobenzoic acid both show relatively high effective organic barriers, but with a substantial difference in (±) bias asymmetry. (b) Perylene-3-COOH and 4-cyanobenzoic acid are dopants which produce strong nonlinear behavior as evidenced by the rapid drop in dynamic resistance.

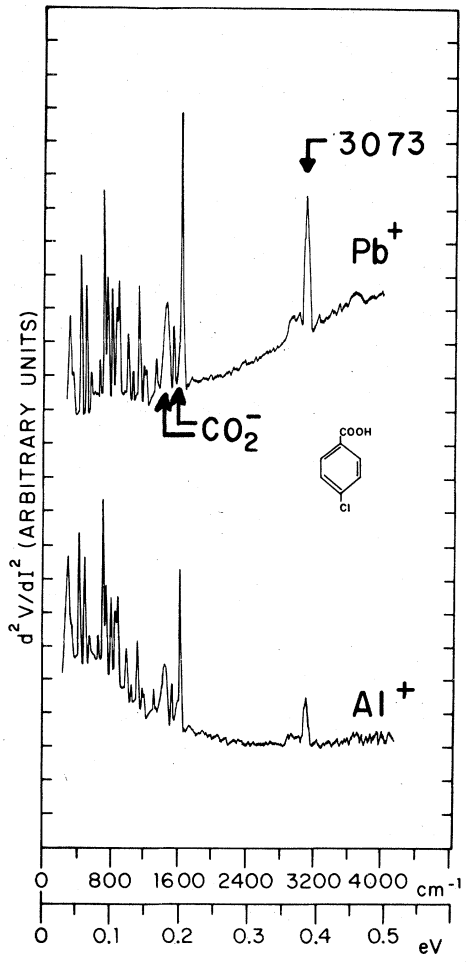

FIG. 3. Inelastic-electron-tunneling (IETS) spectra for 4-chlorobenzoic acid taken for Pb^+ (upper curve) and Al^+ (lower curve). The difference in area under the same mode peak for the two polarities is used to analyze the inelastic asymmetry and to compare it to calculations for the range of the molecular potential.

has been done for all cases and the detailed analysis will be discussed in Sec. IV B.

In addition to the asymmetries in peak intensity the background slope and curvature also show substantial asymmetry. The typical behavior is represented by the chlorobenzoic acid and anthracene-9-carboxylic acid spectra as shown in Figs. 3 and 4. For Pb^+ the overall background slope is positive with upward curvature. For Al^+ the overall slope below 300 meV is negative and becomes slightly positive at higher bias voltages. For both bias voltages broad structure due to the aluminum oxide phonons between 80 and 120 meV contributes to curvature variations in the background of this region. This contribution from the oxide phonons is also observed in the I vs V and dV/dI vs V curves and is generally consistent in all three characteristic curves. For Al^+ the background d^2V/dI^2 shows a reversal of slope in the range 0.2–0.4 V except for the highly nonlinear cases where two reversals of curvature are observed for Al^+.

For dopants which induce strong nonlinear features both the inelastic and the elastic background contributions deviate substantially at high bias voltages. For example 4-cyanobenzoic acid shows a strong reversal of curvature in background slope above 300 meV. For Pb^+ this occurs near 450 meV while for Al^+ it occurs near 300 meV. Inelas-

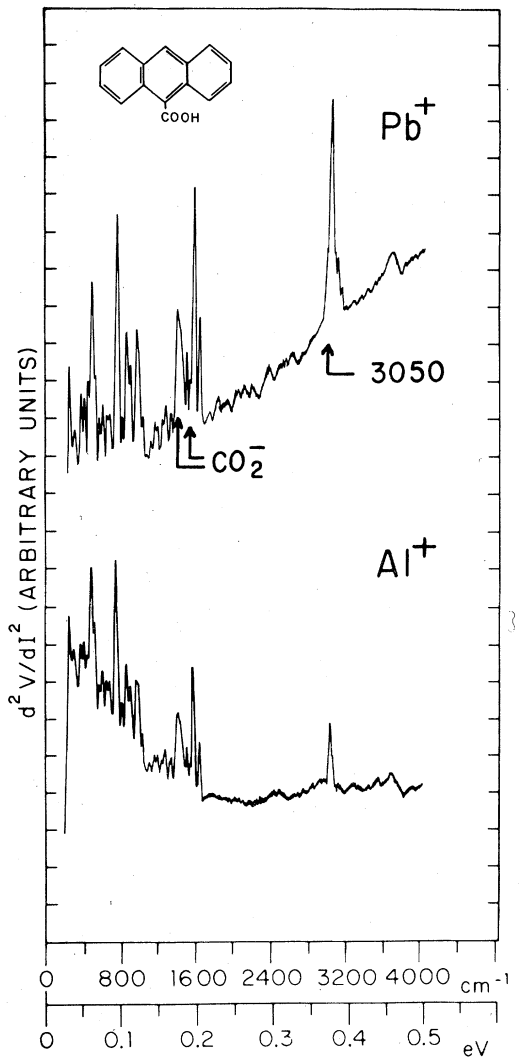

FIG. 4. IETS spectra for anthracene-9-COOH. The two junction polarities Pb^+ (upper curve) and Al^+ (lower curve) are again shown. Both this molecule and the 4-chlorobenzoic acid molecule react with the alumina surface to form a CO_2^- ion which contribute modes as labeled in the upper curves of Figs. 3 and 4. In both cases the C-H stretching mode is located above 3000 cm^{-1} in approximate agreement with the free molecule vibrational spectra.

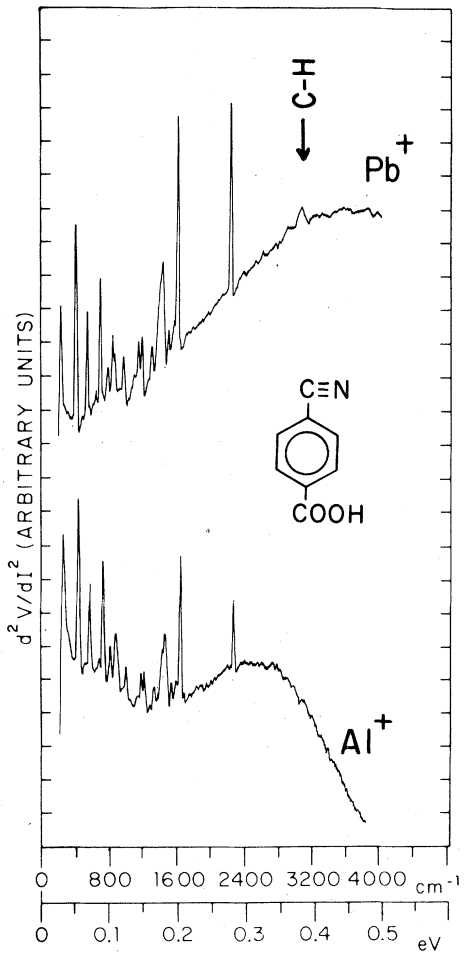

FIG. 5. IETS spectra for 4-cyanobenzoic acid for the two polarities Pb^+ (upper curve) and Al^+(lower curve). The reversal of curvature above 400 meV for Pb^+ and above 300 meV for Al^+ is associated with the very low effective organic barrier height. Modes with higher energies such as the C-H stretching mode are reduced in intensity for organics with low barriers.

tic spectra for 4-cyanobenzoic acid are shown in Fig. 5. As previously observed the onset of this reversal either reduces or eliminates entirely the intensity of the C-H stretching mode at 360 meV. A similar effect is observed in the spectrum of perylene-3-COOH adsorbed on AlO_x as reported in Ref. 7 and shown in Fig. 6.

The inelastic mode intensities and frequencies show quite a few detailed variations associated with the surface-molecular interaction and a number of these have been cataloged in Ref. 7. A significant difference in overall inelastic mode intensity is observed for unsubstituted ring compounds compared to substituted compounds with localized surface interactions. For example the spectra of 4-chlorobenzoic acid and anthracene-9-COOH shown in Figs. 3 and 4 show many extremely intense ring modes while compounds such as anthracene and coronene show much weaker ring mode intensities. A spectrum for coronene is shown in Fig. 7. An additional difference for the spectra of unsubstituted ring compounds shows up as a strong downshift of the aromatic C-H stretching mode normally located above 3000 cm^{-1}. In coronene the mean C-H stretch intensity is observed at 2880 cm^{-1} while in anthracene-9-COOH

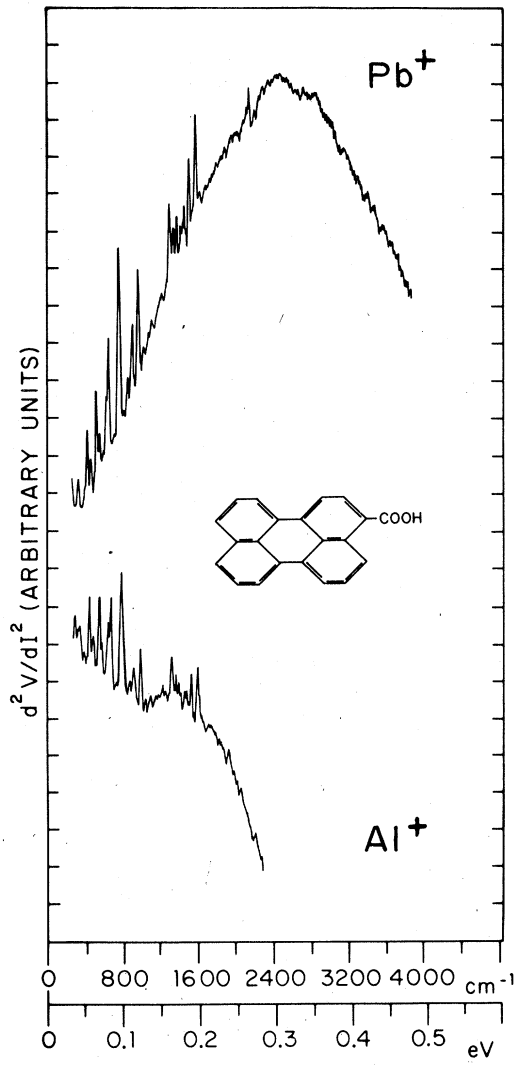

FIG. 6. IETS spectra for perylene-3-COOH. Pb^+ (upper curve); Al^+ (lower curve). The reversal of curvature in this case has an onset at even lower voltage and for the Al^+ polarity reduces the mode intensity for a number of the intermediate phonon modes. This effect gives rise to an enhanced asymmetry in inelastic mode intensity (see Fig. 18).

it is essentially unshifted at 3050 cm^{-1}.

The wide variations in (±) bias asymmetries for both the elastic and inelastic tunneling characteristic plus the changes in mode intensity and frequency observed for the different organic dopants suggest a sensitive dependence of the barrier parameters on the electrode-molecule interface. We have attempted to model the overall elastic characteristics and asymmetries with a two barrier model and a computer fit to the experimental I vs V curves while asymmetries in inelastic mode intensity have been analyzed in terms of the range of the molecular potential interacting with the tunneling electron. Both the models and calculations have lead to fairly consistent fits of the data and the wide variations can be accommodated within the context of a systematic variation of parameters. A summary of the analysis is given in Sec. IV below. Initial details and fits for compounds adsorbed on both AlO_x and MgO have been published in Ref. 7 although the (±) bias asymmetries were not discussed in that paper.

IV. DISCUSSION

A. Barrier models for elastic tunneling

The organic dopants raise the zero-bias resistance of the junctions by at least an order of magnitude and give rise to enhanced nonlinear behavior and (±) bias asymmetries. The organic dopant is itself an insulator and contributes a tunnel barrier with a thickness and height. In addition the molecular charge structure and the organic-metal interface can give rise to changes in the trapezoidal shape of the aluminum oxide barrier.

We have modeled the total barrier with a trapezoidal barrier representing the aluminum oxide and a square barrier representing the organic. The combination barrier is designated TRAPSQR and is diagramed in Fig. 9. In general each barrier will have a different height and thickness and an intrinsic (±) bias asymmetry will be present in the elastic characteristics of the junction. The nonlinear behavior will generally be governed by the effective height of the organic barrier and will be largest when the effective organic barrier height is lowest.

The calculated barrier parameters have been obtained by fitting the experimental I vs V curves using a modified version of the expression given by Brinkman *et al.*[11] based on the WKB approximation and assuming perfectly sharp boundaries between the electrodes and insulator. The current voltage expression is of the form given below[12]:

$$j=\frac{4\pi me}{h^3}\int_0^{E_m}\exp\left(-\frac{\sqrt{8m}}{\hbar}\int_0^{d+s}[\Phi(x,V)-E_x]^{1/2}dx\right)\times dE_x\int_0^{\infty}[f(E)-f(E+eV)]dE_r, \qquad (1)$$

where m is the mass of electron, e is the charge of electron, $\hbar=h/2\pi$ where h is Planck's constant, x is the distance into the barrier, $d+s$ is the total thickness of the barrier, E is the total energy of the electron which equals (E_x+E_r), E_x is the energy component in the x direction of the electron, E_r is the energy component of the electron perpendicular to x, V is the bias voltage applied to junction, (x,V) is the barrier height as a function of x and V, and E_m is the maximum energy in E_x di-

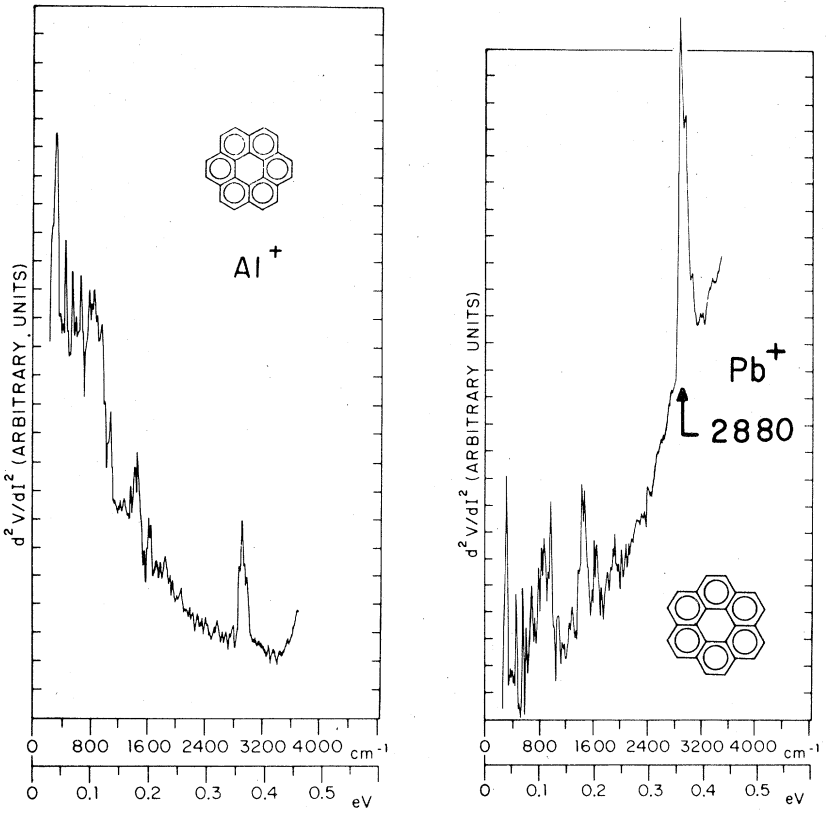

FIG. 7. IETS spectra of coronene. Pb^+ (right curve); Al^+(left curve). The large asymmetry in elastic tunneling shows up as a strong background contribution particularly for the Al^+ spectrum. The C-H stretching mode is downshifted to 2880 cm^{-1} from the free molecule value of 3050 cm^{-1}.

rection of electron.

A linear distribution of voltage across the barrier has been assumed and the potential $\Phi(x, V)$ in Eq. (1) has been expressed in terms of the five barrier parameters for the TRAPSQR barrier shown in Fig. 8.

For left to right tunneling the potential is expressed as

$$\Phi(x,V)=\Phi_1+(\Phi_2-\Phi_1)\frac{x}{d}-\left(\frac{x}{d+s}\right)V+\eta,\quad 0\le x\le d \qquad (2)$$

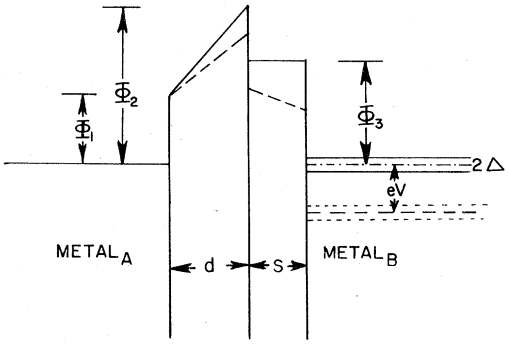

FIG. 8. TRAPSQR barrier used to model the combination aluminum-oxide-organic tunneling barrier. Five parameters have been used, barrier heights Φ_1, Φ_2, Φ_3 and thicknesses d and s.

and

$$\Phi(x,V)=\Phi_3-\left(\frac{x}{d+s}\right)V+\eta,\quad d\le x\le d+s \qquad (3)$$

where η is the Fermi energy of the negatively biased electrode.

For right to left tunneling the potential is expressed as

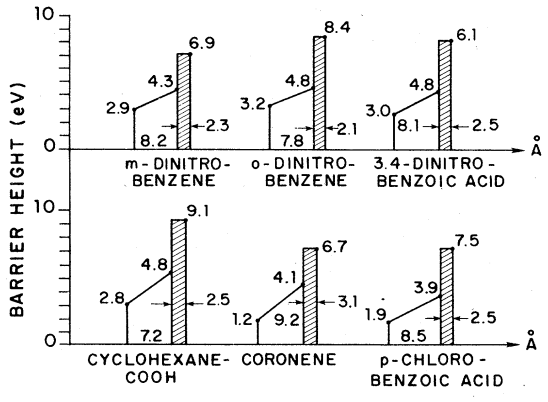

FIG. 9. Representative TRAPSQR barriers resulting from computer fits to Eq. (1) for various organic dopants. These compounds all show relatively high effective organic barrier heights Φ_3.

$$\Phi(x,V)=\Phi_3-\left(\frac{x}{d+s}\right)V+\eta,\quad 0\le x\le s \tag{4}$$

$$\Phi(x,V)=\Phi_2+(\Phi_1-\Phi_2)\frac{x-s}{d}-\left(\frac{x}{d+s}\right)V+\eta,\quad s\le x\le d+s \tag{5}$$

The integration over E_x in Eq. (1) is carried out by a Simpson's rule numerical integration routine with a convergence criterion of 0.1%. A nonlinear least squares routine adapted from Bevington[13] was used on a CDC Cyber 172 computer to vary the parameters in the TRAPSQR model in order to obtain a best fit to the current density versus voltage curve. An initial fit is obtained by varying only Φ_2, Φ_3 and s in order to generate a reasonable set of starting parameters. All five parameters are then allowed to vary and the convergence criterion required χ^2 to vary by less than 1% between successive iterations.

The calculated barriers obtained for a variety of doped junctions are shown in the diagrams of Figs. 9 and 10. The barrier parameters are first calculated for the best fit to the I vs V curves obtained for Al^+ (right to left tunneling) since the greater current rise occurs for this bias. These calculated parameters when substituted into the potential expression for left to right tunneling (Pb^+) also give reasonably good fits to the I vs V curves in all but the extremely nonlinear junctions. As shown in Fig. 11(a) a single set of parameters fits the (±) bias asymmetry observed in coronene with a relatively small error.

Coronene although highly asymmetric has a relatively high effective organic barrier of 6.7 eV and therefore does not show extreme nonlinear behavior. Anthracene-9-COOH is highly asymmetric and also shows a substantial nonlinear behavior for the Al^+ bias with the effective organic barrier height Φ_3 reduced to 3.3 eV and Φ_1 reduced to 0.4 eV. A single set of parameters as shown in Fig. 11(b) again fits both the positive and negative I vs V curves reasonably well although deviation for the higher bias Pb^+ curve is also observed. This deviation for Pb^+ is not fundamental. The Al^+ curve is more nonlinear and therefore more sensitive to the parameter variation and is used to effect the convergence first. Further adjustment could equalize the error, but would not significantly change the parameters. Since the barrier asymmetry of the TRAPSQR model adequately accounts for the asymmetry in two of the highly asymmetric cases the other dopants showing a range of lesser asymmetries are accurately fit with a single set of parameters. For example 3,4-dinitrobenzoic acid as shown in Fig. 12(b). The model barriers

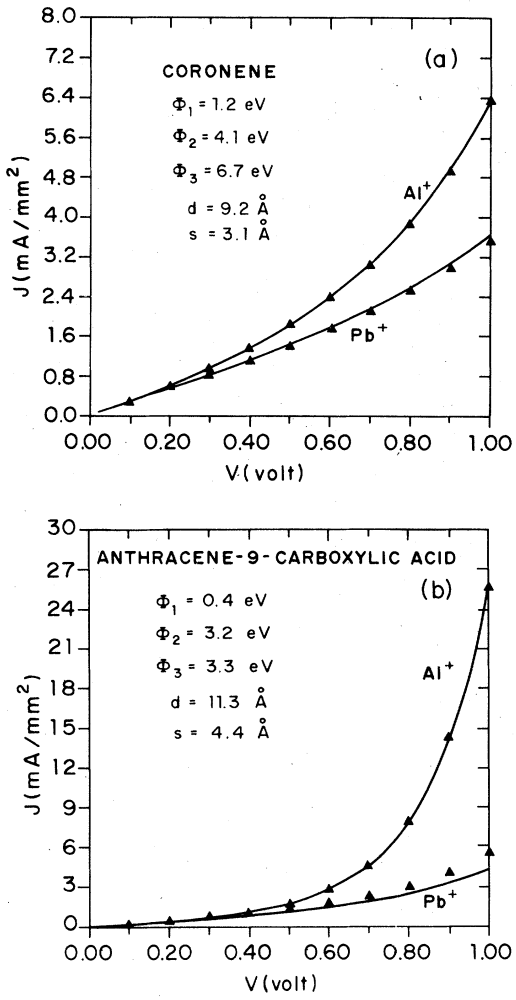

FIG. 11. Computer fits to the experimental I vs V data on coronene (a) and anthracene-9-carboxylic acid. (b) Solid curves are the calculated curves and the solid triangles are the data points. Both the Pb^+ and Al^+ polarities have been fit with the same set of parameters as listed. In both cases the elastic tunneling asymmetry is accounted for by the calculated barrier shape.

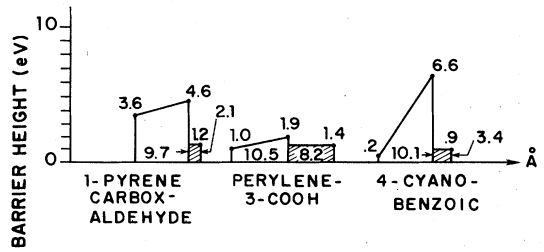

FIG. 10. Calculated barriers for three dopant compoounds which show low effective barrier heights, strong linear behavior and large asymmetries at high bias voltages. The overall barrier shapes in these cases are quite variable.

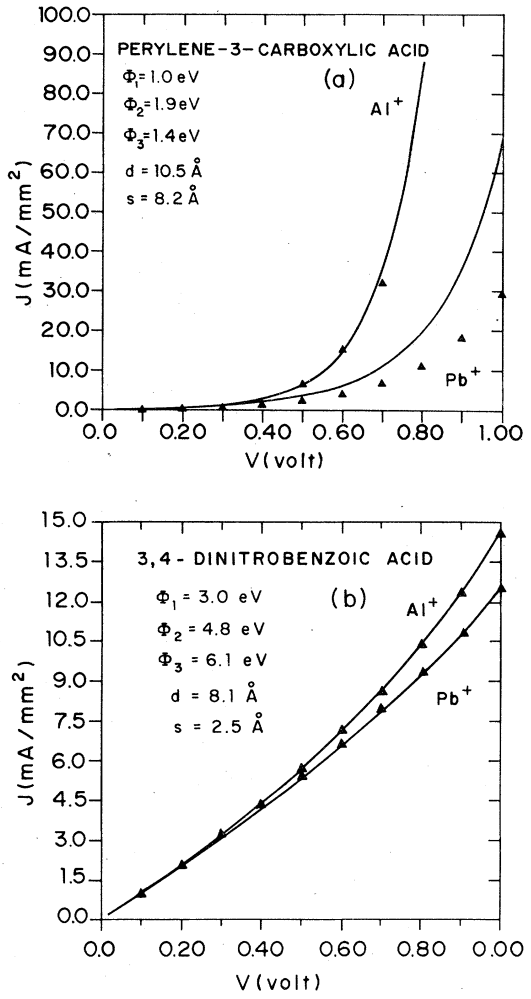

FIG. 12. (a) Computer fits to the I vs V data for the highly asymmetric and nonlinear behavior observed for the perylene-3-carboxylic acid dopant. In this case Al^+ data is fit well by the set of barrier parameters indicated, but the Pb^+ data corresponds to a greater asymmetry than can be accounted for within the TRAPSQR model. (b) Computer fit to 3,4-dinitrobenzoic acid which shows a very symmetric (±) bias behavior.

which result from junctions doped with compounds that give high effective organic barriers are all similar in shape (see Fig. 9) and correspond to a solution of Eq. (1) which fits both the current and (±) bias asymmetry well.

For the highly nonlinear junctions the asymmetries become extreme at high bias voltages and it is difficult to fit I vs V curves for both (±) bias with the same set of parameters. In these cases the effective organic barrier height is generally reduced to the range of 1 eV or less and the other barrier parameters are also lowered. Typical fits for perylene-3-COOH are shown in Fig. 12(a). The parameter convergence has again been obtained using the Al^+ data. With these parameters substituted in the potential expression for Pb^+ a large asymmetry accounting for 80%–90% of the observed asymmetry is obtained, but the calculated current is still too large as indicated by the lower curve and points of Fig. 12(a).

The extreme nonlinear junctions are consistently modeled with lower barrier heights and effectively thicker organic barriers. However, the detailed shapes and relative heights of the oxide and organic barriers become more variable and it is more

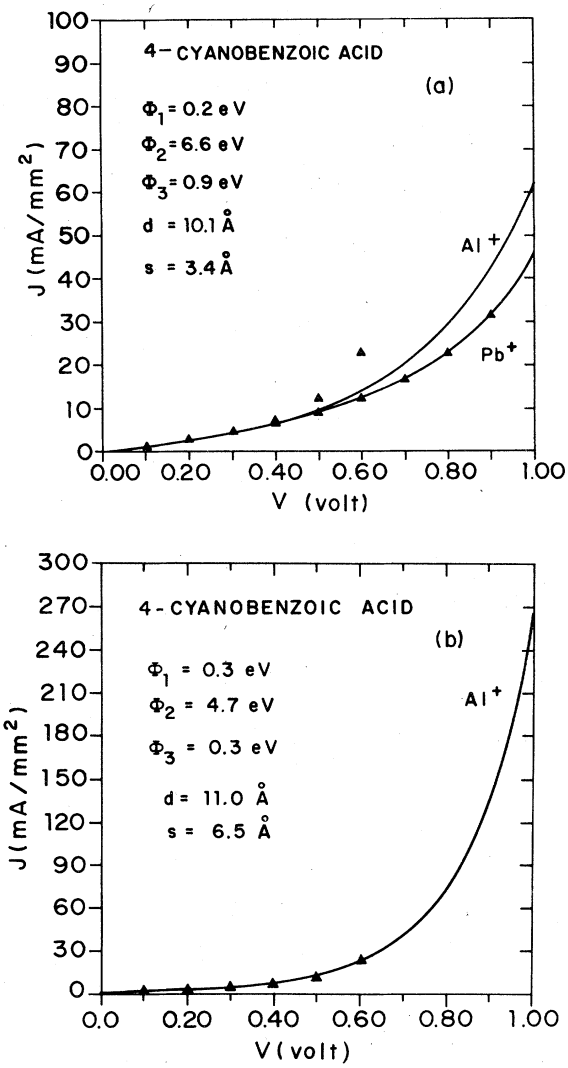

FIG. 13. Computer fits to I vs V data for 4-cyanobenzoic acid. The Pb^+ and Al^+ curves can be fit with different sets of parameters as indicated in (a) and (b). However as shown in (a) the (±) bias asymmetry cannot be adequately fit. This is again connected with the extreme nonlinear behavior associated with the low-effective organic barrier.

difficult to obtain a unique set of parameters. The asymmetries cannot be fully accounted for with a single TRAPSQR barrier shape and slower convergence for fits to the I vs V curves is observed. Typical barrier shapes for the dopants giving low effective organic barrier heights were shown in Fig. 10. For example junctions doped with 4-cyanobenzoic acid show the most extreme nonlinear behavior and (±) bias asymmetry. The combination barrier is characterized by an extremely low organic barrier and an enhanced trapezoidal shape for the oxide barrier. As shown in Fig. 13 this shape can fit both the Al^+ and Pb^+ data but with somewhat different values of the parameters. However, for either set of parameters the (±) bias asymmetry is not adequately accounted for as indicated in Fig. 13(a) for the Al^+ data calculated with the Pb^+ parameters. In the case of perylene-3-COOH a more regular barrier was obtained, but all barrier heights were low making it difficult to predict the full asymmetry.

The reason for the wide range of effective barrier heights and shapes due to the different dopants is yet to be fully understood. Several observations can be made on this point although detailed mechanisms have to remain speculative. Drastic modifications of the adsorbed molecules do not take place since in most all cases the majority of the vibrational modes can be quite accurately matched against the Raman and infrared spectra of the unperturbed molecule. Different orientations of the rings on the surface are possible and are influenced by reactive side groups. For example molecules with a COOH substituent react with the AlO_x surface by donating a proton and forming a CO_2^- carboxylate ion[14,15] with a symmetric bidentate structure and equivalent oxygen atoms. Anthracene-9-COOH is such a case and the aromatic rings are probably held off the surface. In contrast coronene is a planar ring structure and would be expected to lie flat on the surface. The π electrons may then form some degree of complex with the surface and a related downshift of the C-H stretching mode occurs.

The above two cases show markedly different inelastic mode intensities and similar cases have been compared in Refs. 6 and 7. For unsubstituted ring compounds like coronene the ring modes generally show low intensity and the inelastic-electron-tunneling (IETS) spectra are dominated by the modes with predominately CH character. Ring compounds substituted with a COOH group generally show much stronger IETS intensity and in all cases the COOH interacts with the alumina to form a carboxylate ion. The IETS spectra for these compounds are characterized by a number of very strong ring modes involving stretch motions of the ring carbon atoms. The difference in IETS mode intensities observed for the two classes of compounds described above suggest subtle changes in the electronic interaction with the surface accompanied by changes in the strength of the inelastic coupling to the phonon modes. These changes in inelastic mode intensity do not seem to be correlated with any major changes in the model barrier parameters or the differences observed in the elastic behavior. For example coronene and anthracene-9-COOH produce effective organic barrier heights of 6.7 and 3.2 eV, respectively. Although they differ by a factor of 2 both are relatively high and both show a strong (±) bias asymmetry adequately modeled by the TRAPSQR barrier as indicated in Fig. 11. Therefore from the elastic tunneling characteristics the two molecules produce similar behavior while the inelastic modes indicate a substantial difference in surface interaction.

In contrast to anthracene-9-COOH perylene-2-COOH shows more nonlinear elastic behavior, much less asymmetry and a low effective organic barrier height (1.2 eV). This major difference of barrier shape and height must therefore involve a combination of the COOH interaction with the surface and the electronic structure of the ring complex. This must arise from rather subtle differences in net molecular charge and π-electron density since the basic molecular structure interacted on the surface would not be expected to be drastically different.

The inelastic mode intensity asymmetries give information on the range of the molecular potential and the analysis of this asymmetry is discussed below. A large number of cases representing the complete range of elastic behavior have been analyzed in order to look for possible changes in the behavior of the molecular–tunneling-electron interaction potential.

B. Asymmetry in inelastic peak intensity

The dopant molecules are adsorbed on one side of the aluminum oxide barrier and are therefore spatially asymmetric with respect to left-right versus right-left tunneling electrons. For the inelastic electron tunneling channel this can introduce a difference in barrier transmission for left-right versus right-left tunneling since for one polarity the electron loses energy after tunneling and for the other polarity loses energy before tunneling. The tunneling probability is proportional to energy and one would therefore expect a greater inelastic tunneling current with the lead electrode positive (left-right tunneling). The size of this inelastic mode intensity asymmetry will also depend on the

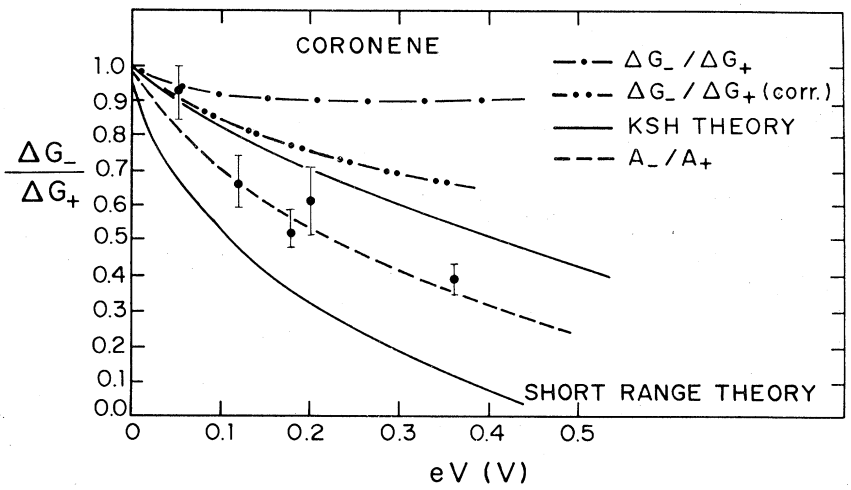

FIG. 14. Data and analysis showing the (±) bias asymmetry in conductance change, ΔG, associated with vibrational mode excitation by IETS in coronene. The points represent ratios of the areas under a given mode peak in the d^2V/dI^2 vs V spectrum measured for opposite bias voltage on the junction. (+) refers to Pb^+ and (−) refers to Pb^-. The dashed curve is the best fit through the points representing the area ratios. The curves labeled $\Delta G_-/\Delta G_+$ and $\Delta G_-/\Delta G_+$ (corrected) are the conductance change ratios computed from the measured area ratios. The final curve to be compared to theory is corrected for the elastic asymmetry G^-/G^+. The lowest solid curve represents a short range potential interaction calculated in Ref. 16 while the upper solid curve represents a long range potential interaction calculated in Ref. 4. After correcting for the large conductance asymmetry observed in coronene the conductance change asymmetry associated with the vibrational modes falls close to that predicted by KSH.

range of the potential describing the interaction between the tunneling electron and the molecule. If the potential range is comparable or greater than the barrier thickness the effect will be reduced while if a very short range molecular potential is appropriate a maximum asymmetry should be observed.

The expected asymmetry has been calculated for a number of cases. Yanson *et al.*[16] assumed a δ function potential at the electrode-molecule interface and calculated the asymmetry in conductance ($\Delta G_-/\Delta G_+$) as shown by the lowest curve in Fig. 14. Kirtley, Scalapino, and Hansma[4] used a longer range Coulomb potential with partial charges representing the bound electrons of the molecule. Assuming that the molecule extends ~1 Å beyond the effective electrode-barrier interface they calculated the asymmetry as shown by the upper solid curve in Fig. 14 and referred to as KSH.

The exact potential has both a short range molecular part and a longer range dipole part. Kirtley and Soven[17] have developed a short-range multiple

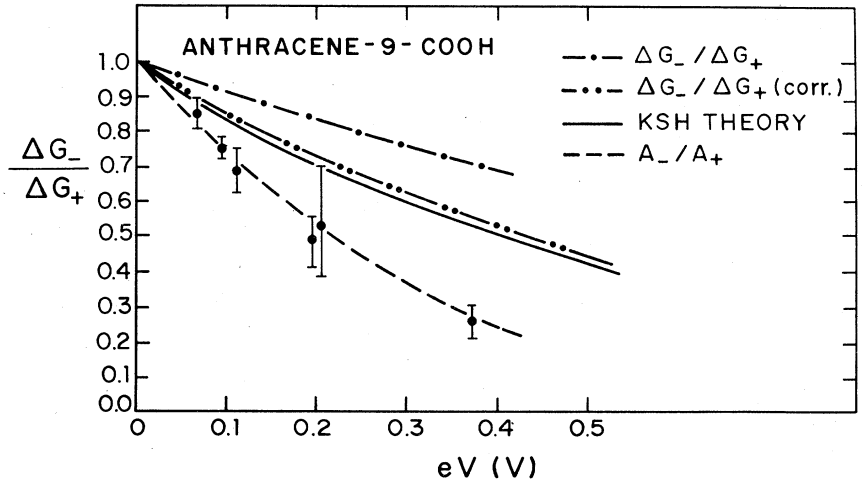

FIG. 15. ΔG asymmetry associated with inelastic peak intensity for anthracene-9-COOH. See Fig. 14 for definitions of the curves. The final corrected asymmetry curve is very close to that predicted by KSH for long-range theory.

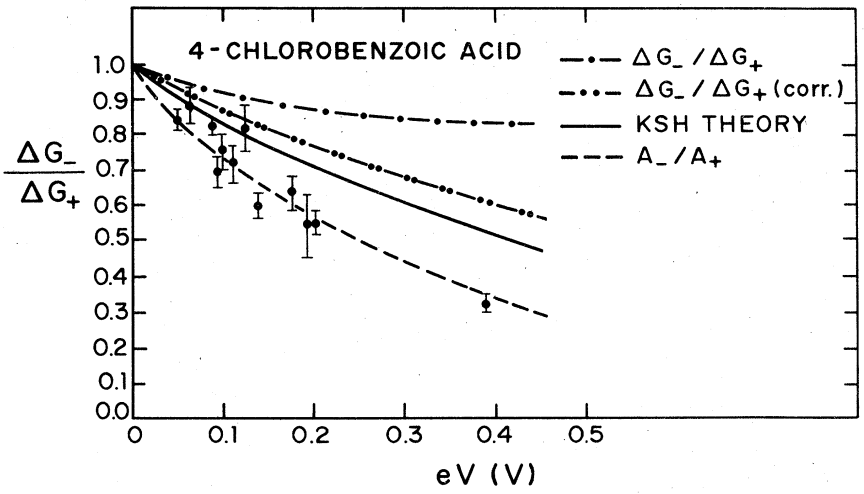

FIG. 16. ΔG asymmetry associated with the inelastic mode intensity for 4-chlorobenzoic acid. This is very similar to the behavior for anthracene-9-COOH and is typical of all compounds measured which have fairly large effective organic barrier heights.

scattering theory of IETS intensities using an $X\alpha$ approximation for the exchange correlation potential and a Bardeen transfer Hamiltonian approach to calculate inelastic tunneling cross sections. They calculate higher harmonic amplitudes and opposite voltage bias asymmetries for the specific case of CO adsorbed in a Al-AlO$_x$-Rh-CO-Pb junction. For this case they predict a large asymmetry ratio which would not be far from that predicted by the δ-function potential. The predicted short-range cross sections are strongly energy dependent and could become quite large if the tunneling electron happened to correspond to a molecular bound state energy. Such a resonance scattering state might be important for particular molecules although results to date on IETS suggest that the long-range potential is dominant. This is the case for benzoic acid on alumina as reported by Kirtley *et al.*[4]

We have examined a large number of junctions doped with different organics and have analyzed the experimental (±) bias asymmetries in inelastic intensity for possible variations. These have included dopants which produce the complete range of barrier behavior outlined in Secs. III. We have also looked at several dinitrobenzoic acids since dinitro compounds are reported to show the longest negative ion resonant lifetimes.[18]

Since the quantity needed for comparison to theory is the conductance change ΔG associated with the inelastic event the area under the observed peak in d^2V/dI^2 is measured and then converted using the calibrated conductance of the junction and the relation

$$\frac{d^2I}{dV^2} = -\frac{1}{G^3}\frac{d^2V}{dI^2}. \tag{6}$$

Selected peaks have been analyzed for both (±) bias and the ratio $\Delta G^-/\Delta G^+$ is then plotted as a function of voltage as shown in Figs. 14–19. The theoretical curves of Fig. 14 were calculated assuming the

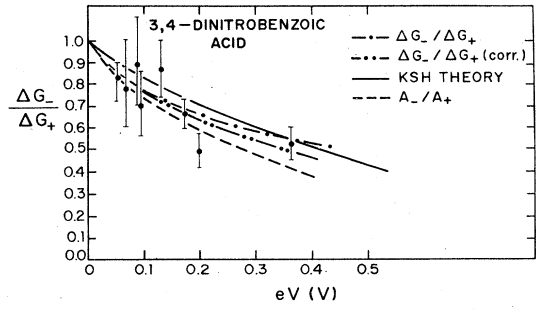

FIG. 17. ΔG asymmetry associated with the inelastic peak intensity for 3,4-dinitrobenzoic acid. The elastic conductance is quite symmetric for this dopant so that the calculated curves group together. The final asymmetry is again not far from KSH. No evidence of resonance effects is observed although the free molecule is expected to show a long negative ion resonance lifetime.

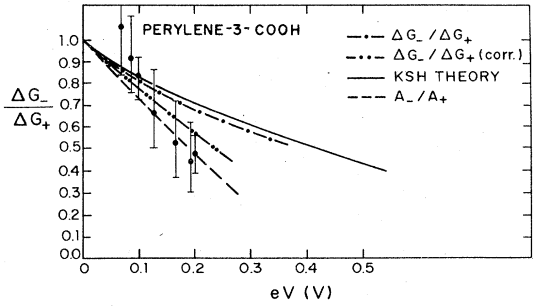

FIG. 18. ΔG asymmetry associated with the inelastic peak intensity for perylene-3-COOH. In this case the asymmetry is greater than predicted by the long range potential interaction of KSH. This additional asymmetry is correlated with the low barrier height and curvature reversal in d^2V/dI^2 vs V and is not necessarily connected with the molecular potential range.

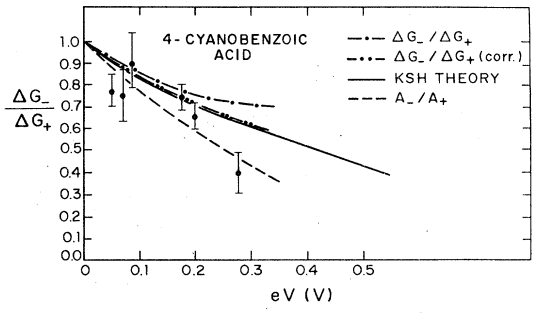

FIG. 19. ΔG asymmetry associated with the inelastic peak intensity for 4-cyanobenzoic acid. In this case the curvature reversal in d^2V/dI^2 vs V is well above the lower lying phonon modes which again show a ΔG asymmetry close to that expected from KSH.

tunnel barrier to be square and hence takes no account of the barrier asymmetry introduced by the organic or dissimilar metal electrodes. Such a calculation would be rather complex so that only an approximate correction can be made at this time. The measured ratio $\Delta G^-/\Delta G^+$ has a contribution from both the molecular potential range effect and the direct barrier asymmetry one measure of which is the ratio G^-/G^+. The conductance G^- is always greater than G^+ consistent with the barrier shape which makes it easier to tunnel from right to left and therefore counters the potential range asymmetry (molecules are located on the right side). An approximate correction for this effect can be made by simply multiplying the ratio $\Delta G^-/\Delta G^+$ by G^+/G^- which approximately cancels the effect of the barrier asymmetry. The final experimental curve converted to $\Delta G^-/\Delta G^+$ and corrected for conductance asymmetries is labeled $\Delta G^-/\Delta G^+$ (corrected) in Figs. 14–19 and is the one that should be compared to the calculated curve labeled KSH. The original asymmetries in areas measured from the d^2V/dI^2 vs V curve are represented by the points. The dashed curve is the best fit through the experimentally measured points.

Although the experimental scatter for a given junction is fairly large comparison of the results on the entire range of junctions shows a systematic trend. In most cases the inelastic asymmetry is close to that predicted by the KSH theory using the long range potential. Large differences in elastic asymmetry and the apparent differences in measured d^2V/dI^2 inelastic peak asymmetry generally cancel out in the final corrected quantity which measures the true potential range asymmetry of the inelastic tunneling channel.

Figures 14 and 15 show results on coronene and anthracene-9-COOH. These are dopants which give high effective organic barriers and show substantial (±) bias asymmetries in the elastic characteristics. They also represent the two different cases of strong and weak inelastic coupling to the major ring vibrations which may be related to differences in surface interaction. The direct data when converted to $\Delta G_-/\Delta G_+$ give the upper curves in Figs. 14–19 and show the effect of the large conductance asymmetry which counters the asymmetry produced by the potential interaction. The final curves $\Delta G_-/\Delta G_+$ (corrected) with the effect of the conductance asymmetry approximately removed give inelastic intensity asymmetries which are not far from those calculated by KSH. A single ring compound like 4-chlorobenzoic acid also gives a very similar result as shown in Fig. 16. The results on 3,4-dinitrobenzoic acid show much less intrinsic (±) bias asymmetry in the elastic tunneling and barrier shape and therefore the corrections are smaller. However, the observed inelastic asymmetry as shown in Fig. 17 is again close to that calculated by KSH with no evidence of enhanced asymmetry due to possible short range potential effects and resonance.

The molecules like perylene-3-COOH and 4-cyanobenzoic acid which produce very low effective organic barriers have also been analyzed for (±) bias asymmetries in inelastic intensity. For perylene-3-COOH which was characterized by a curvature reversal in d^2V/dI^2 below 300 meV and a corresponding loss of intensity in the C-H stretching mode the asymmetry in mode intensity is stronger than predicted by KSH as shown in Fig. 18. Since the change in curvature and loss of intensity in the vibrational modes is itself quite asymmetric (see Fig. 7) the enhanced inelastic intensity asymmetry can be directly correlated with this behavior. Whether this is related in turn to the molecular potential is not clear at this time.

4-cyanobenzoic acid exhibits the same type of d^2V/dI^2 curvature reversal but at higher bias voltage (~500 meV for Pb^+, see Fig. 6). This is sufficiently above most of the phonon peak energies such that the inelastic peak intensity asymmetry below the C-H stretching mode is apparently unaffected as shown in Fig. 19 and again agrees with KSH.

V. CONCLUSIONS

Measurements and analysis of the characteristic tunneling curves for Al-AlO_x-Pb tunnel junctions doped with a wide range or organic ring compounds have been carried out. These dopants have been selected on the basis of substantial variations in the effect of the dopant on both the elastic and inelastic characteristics of the junctions. In this study we have analyzed particularly the (±) bias asymmetries appearing in both the elastic and in-

elastic tunneling components.

The elastic tunneling current vs voltage and the (±) bias asymmetry in the elastic tunneling characteristic can be adequately modeled with a modified version of standard tunneling equations. We have modeled the barrier in two parts, a trapezoid representing the oxide and a square barrier representing the organic. The effective organic barriers vary from less than 1 eV to 9 eV and produce a wide variation in the elastic tunneling observed in the bias range 0–1 V. In most cases the model is adequate for obtaining a reasonably good fit to both the Pb^+ and Al^+ characteristic curve with a single set of parameters describing the barrier.

The most unusual behavior occurs for the compounds which produce very low effective organic barriers. These show a curvature reversal in the d^2V/dI^2 vs V curve above some critical bias and this enhances the asymmetry in both the elastic and inelastic tunneling components.

The (±) bias asymmetries in the inelastic peak intensities have also been measured and analyzed for the same range of compounds. The results have been compared to calculated asymmetries based on the range of the molecular potential tunneling electron interaction. After correcting for the wide variations in elastic conductance asymmetry we conclude that for most of the compounds the intensity asymmetry follows that expected for a long-range potential interaction. Stronger asymmetries have been observed for those compounds showing extremely low effective organic barrier heights and this is related to the correlated effects of curvature reversal in d^2V/dI^2 vs V and loss of mode intensity.

The origin of the interface structure providing these low effective barrier heights and the correlated effects on the inelastic tunneling interaction needs further investigation. They are reproducible and occur for a rather selected group of molecules although no single structural feature clearly distinguishes each case. Preliminary data with other oxides and electrodes indicates that all elements of the interface and barrier play a role.

Although a still wider range of organic molecules should be studied no case has yet been found where the inelastic intensity asymmetry is large enough to suggest short range potential interactions or resonance. Dinitro compounds where negative ion resonances are long lived do not show enhanced asymmetry although the surface adsorbed molecule is of course not necessarily comparable to the free molecule.

The tunneling data presented here have shown that the interface structure and effective barriers in these doped junctions exhibit significant variations related to surface molecular interactions. The microscopic models need to be developed, but the sensitivity of the technique to interface structure looks promising.

ACKNOWLEDGMENTS

This research has been supported by the U. S. Department of Energy. The authors have had useful discussions with Professor P. K. Hansma, Professor D. J. Scalapino, Professor J. M. Rowell, Professor V. Celli, Professor C. H. Lochmüller, and Professor J. W. Mitchell. Professor O. R. Rodig has helped with various aspects of the chemical preparation. Estelle Phillips has made valuable contributions to the measurement and fabrication of the tunnel junctions. James Lau and Andrew Johnson have contributed to various aspects of the experiment.

[1]J. Lambe and R. C. Jaklevic, Phys. Rev. 165, 821 (1968).
[2]M. G. Simonsen, R. V. Coleman, and P. K. Hansma, J. Chem. Phys. 61, 3789 (1974).
[3]D. J. Scalapino and S. M. Marcus, Phys. Rev. Lett. 18, 459 (1967).
[4]J. Kirtley, D. J. Scalapino, and P. K. Hansma, Phys. Rev. B 14, 3177 (1976).
[5]J. G. Simons, Phys. Rev. Lett. 10, (1963).
[6]C. S. Korman and R. V. Coleman, Phys. Rev. B 15, 1877 (1976).
[7]C. S. Korman, J. C. Lau, A. M. Johnson, and R. V. Coleman, Phys. Rev. B 19, 994 (1979).
[8]M. G. Simonsen and R. V. Coleman, Phys. Rev. B 8, 5875 (1973).
[9]P. K. Hansma and R. V. Coleman, Science 184, 1369 (1974).
[10]J. G. Adler, T. T. Chen, and J. Straus, Rev. Sci. Instrum. 42, 362 (1971).
[11]W. F. Brinkman, R. C. Dynes, and J. M. Rowell, J. Appl. Phys. 41, 1915 (1970).
[12]J. G. Simmons, J. Appl. Phys. 34, 1793 (1963).
[13]P. R. Bevington, *Data Reduction and Error Analysis for the Physical Sciences* (McGraw Hill, New York, 1969).
[14]J. T. Hall and Paul K. Hansma, Surf. Sci. 76, 61 (1978).
[15]J. T. Hall and Paul K. Hansma, Surf. Sci. (to be published).
[16]I. K. Yanson, N. I. Bogatina, B. I. Verkin, and O. I. Shklyarevskii, Sov. Phys. JETP 35, 540 (1972).
[17]J. Kirtley and P. Soven, Phys. Rev. B 19, 1812 (1979).
[18]J. P. Johnson, L. G. Christophorou, D. L. McCorkle, and J. G. Carter, J. Chem. Soc. Faraday Trans. II 71, 1742 (1975).